Electrochimica Acta 76 (2012) 88–93

Contents lists available at SciVerse ScienceDirect

Electrochimica Acta

journal homepage: www.elsevier.com/locate/electacta

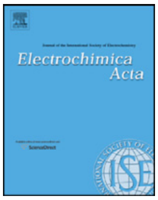

The influence of the Pt crystalline surface orientation on the glycerol electro-oxidation in acidic media

Janaina Fernandes Gomes*, Fernanda Batista Castelo de Paula, Luiz Henrique S. Gasparotto, Germano Tremiliosi-Filho

Instituto de Química de São Carlos, Universidade de São Paulo, C.P. 780, 13560-970 São Carlos, SP, Brazil

ARTICLE INFO

Article history:
Received 1 February 2012
Received in revised form 9 April 2012
Accepted 14 April 2012
Available online 14 May 2012

Keywords:
Glycerol oxidation
Single crystal Pt surfaces
Acid medium
Reaction intermediates and products formation

ABSTRACT

We investigated the electrochemical oxidation of glycerol on low-index Pt single crystals in acidic media (H_2SO_4 and $HClO_4$) by cyclic voltammetry and Fourier Transform Infrared (FTIR) spectroscopy and we verified that this is a surface sensitive reaction. Pt(1 0 0) and Pt(1 1 0) surface structures favor the breaking of the C—C—C bond at low potentials (say 0.05 V), as seen by the formation of CO, one of the adsorbed residues of the glycerol dissociation, which poisons these surfaces even at high potentials. Pt(1 1 1) surface structure does not favor the C—C—C bond breaking at potentials as low as 0.05 V. However, Pt(1 1 1) is less poisoned by residues of glycerol dissociation and, for this reason, it is more active for glycerol oxidation than Pt(1 0 0) and Pt(1 1 0) at low potentials. Carbonyl containing compounds and CO_2 were detected as reaction products of the glycerol oxidation on all investigated single-crystal Pt surfaces. The ratio between CO_2 and carbonyl containing compounds is clearly much higher for Pt(1 0 0) and Pt(1 1 0) than for Pt(1 1 1).

1. Introduction

Nowadays, glycerol is abundantly produced as a co-product of the biodiesel fabrication and its application is mainly restricted to raw material for pharmaceutical and cosmetics industries. As a result, the offer of this alcohol surpasses its actual demand and the accumulation of big volumes of glycerol can become an environmental problem in a short timescale. For this reason, there has been an effort in finding new applications for glycerol. One of the possibilities is the application of glycerol in direct glycerol fuel cells for electric energy generation and co-generation of commercially interesting chemicals, such as dihydroxyacetone [CH_2OH—(C=O)—CH_2OH], which is used as an ingredient in sunless tanning products.

At present, some difficulties related to practical catalysts (usually metallic particles dispersed in carbon powder) make unfeasible the application of glycerol in direct glycerol fuel cells. One of the difficulties is to control the selectivity of the glycerol oxidation reaction towards the desired chemicals. Another difficulty is the formation of poisoning adsorbed intermediates on the catalyst surface at low overpotentials. In order to overcome these difficulties, studies on the electro-oxidation of glycerol on model surfaces, for example Au and Pt single crystals, are fundamental to unravel the mechanism of this process. These studies supply us with information about the role of the surface crystallographic orientation on the catalytic electro-oxidation of glycerol. Based on this knowledge, practical catalysts with specific sites can be designed to improve the electrochemical process for fuel cell application with co-generation of chemicals.

Glycerol reacts on metal surfaces through a complex mechanism that leads to the formation of a large variety of final reaction products, including compounds with one, two, and three carbon atoms [1–6]. In particular, glyceraldehyde (CH_2OH—CHOH—CHO), dihydroxyacetone [CH_2OH—(C=O)—CH_2OH], glyceric acid (CH_2OH—CHOH—COOH), tartronic acid (COOH—CHOH—COOH), glycolic acid (COOH—CH_2OH), glyoxylic acid (COOH—CHO), formic acid (HCOOH) and carbon dioxide (CO_2) were detected as solution phase reaction products of the glycerol oxidation on Pt in acidic medium [7–11]. The variety of incomplete oxidation products with the C—C bonds remaining intact or only partly broken points to pronounced kinetic limitations for the dissociative adsorption and subsequent complete oxidation of glycerol to CO_2. Details of the reaction mechanism of glycerol oxidation on Pt surfaces, however, are still largely unknown. In order to gain a better insight into the electrochemical reactivity of glycerol, detailed studies about glycerol adsorption and oxidation are necessary with the aim of identifying the main species involved in the different steps.

The electro-oxidation of alcohols, such as methanol and ethanol, on metallic single crystals has been extensively investigated and the effect of the surface crystallographic orientation

---

* Corresponding author. Tel.: +55 16 3373 9934; fax: +55 16 3373 9952.
E-mail address: janainafg@iqsc.usp.br (J.F. Gomes).

0013-4686/$ – see front matter © 2012 Elsevier Ltd. All rights reserved.
http://dx.doi.org/10.1016/j.electacta.2012.04.144

on these reactions is well-established [12–20]. Differently, the electro-oxidation of glycerol over these model catalysts has been scarcely investigated and not much is known about the influence of surface structure on the oxidation of glycerol [2,21]. In the present work, we investigate the electrochemical oxidation of glycerol on low-index Pt single crystals in acidic media (H_2SO_4 and $HClO_4$) by cyclic voltammetry and Fourier Transform Infrared (FTIR) spectroscopy. This study provides us with additional information on the structural sensitivity of the electro-oxidation of glycerol.

2. Experimental

2.1. Experimental conditions, reactants and instrumentation

All the experiments were performed at room temperature (25 ± 1 °C). The chemicals used for solution preparations were high-purity sulfuric acid (Merck suprapur®), perchloric acid (70%, Sigma–Aldrich), glycerol (J.T. Baker), and ultrapure water from Millipore system. The counter electrode was a 1 cm × 1 cm Pt foil. The reference electrode was a reversible hydrogen electrode (RHE) and all potentials in this work are referred to it. The working electrodes were Pt(1 1 1), Pt(1 0 0) and Pt(1 1 0) discs (10 mm diameter × 2 mm thick) acquired from MaTeck.

The experiments were carried out with a 1285 Solartron potentiostat/galvanostat controlled by the CoreWare software. The FTIR instrument was a Nicolet Nexus 670 spectrometer equipped with a liquid nitrogen cooled MCT detector. *In situ* FTIR experiments were performed in a three electrode spectro-electrochemical cell with a planar ZnSe window attached to the bottom of the cell. ZnSe is one of the most popular materials for infrared applications due to its very wide infrared transparent range covering 4000–650 cm^{-1}. The planar shape of the ZnSe window was chosen in order to fit the design of our spectro-eletrochemical cell. Details concerning the cell are described elsewhere [22]. Briefly, a movable piston supports the working electrode. A platinum wire connected to the working electrode passes through the piston and keeps the electric contact. The ZnSe window functions as a transparent cover for the cell and, also, as a wall against which the working electrode is pressed to obtain a thin film of electrolytic solution. In such a way, the absorption of the infrared beam by the solution is minimized during the FTIR measurements. For all three surfaces, the angle of incidence of the IR beam was kept constant at 65°.

2.2. Experimental procedure

In order to have ordered and clean surfaces, the working electrode was heated in a hydrogen–oxygen flame and cooled down in a reductive H_2 + Ar atmosphere. In sequence, the electrode was protected with a waterdroplet saturated with cooling gases to prevent the contamination and reconstruction of the surfaces during the transfer to the spectro-electrochemical cell. The working electrode was then introduced into the cell containing oxygen-free working solutions (0.1 mol L^{-1} H_2SO_4, 0.1 mol L^{-1} $HClO_4$, 0.1 mol L^{-1} H_2SO_4 + 0.1 mol L^{-1} glycerol or 0.1 mol L^{-1} $HClO_4$ + 0.1 mol L^{-1} glycerol) at 0.05 V *vs.* RHE. In the sequence, cyclic voltammetry or FTIR spectroscopy (first series of increasing potential steps) was performed. The order of the Pt single crystals and the cleanliness of the electrolytic solution were tested by the stability of the characteristic voltammetric features of the Pt single crystals in pure electrolyte (0.1 mol L^{-1} H_2SO_4 or 0.1 mol L^{-1} $HClO_4$) using a meniscus configuration. Cyclic voltammograms were obtained in the potential range between 0.05 V and 0.8 V for Pt(1 0 0) and Pt(1 1 0) and between 0.05 V and 0.9 V for Pt(1 1 1). The superior potential limits were set to avoid the irreversible anodic oxide formation that lifts the reconstruction of the Pt single crystals. FTIR spectra were taken in the wavenumber region between 4000 cm^{-1} and 800 cm^{-1}, in the potential ranges mentioned above, in 0.10 V steps. Spectra were computed from the average of 128 interferograms. The spectral resolution was set to 8 cm^{-1}.

Reflectance spectra were calculated as the ratio (R/R_o), where R represents a spectrum at the sample potential and R_o is the spectrum collected at 0.05 V. Positive and negative bands represent the consumption and the production of substances at the sample potential, respectively.

In order to compare the activity of the Pt single crystals for the glycerol oxidation in acidic media, the faradaic currents were normalized by Pt active surface areas. These areas were determined with basis on the cyclic voltammograms of the Pt single crystals in the supporting electrolyte (0.1 mol L^{-1} H_2SO_4 or 0.1 mol L^{-1} $HClO_4$). The active surface area was calculated by integrating the faradaic current related to the hydrogen/anion desorption. The faradaic charges of a hydrogen monolayer on Pt(1 1 1), Pt(1 0 0), and Pt(1 1 0) are assumed to be 241 $\mu C\,cm^{-2}$, 212 $\mu C\,cm^{-2}$, and 220 $\mu C\,cm^{-2}$, respectively [23–25]. The roughness factor (ratio between active area and geometric area) of Pt(1 1 1), Pt(1 0 0), and Pt(1 1 0) is 1.0, 1.1 and 1.0, respectively.

All the experiments were made in duplicate and the results were reproducible in the limit of the experimental error.

3. Results and discussion

3.1. A general mechanism of glycerol electro-oxidation on Pt in acidic medium

With basis on the current knowledge of the electro-oxidation of glycerol on Pt in acidic media [7,9–11], a general reaction mechanism can be formulated as follows:

$$\underset{\text{glycerol}}{H_2C(OH)\text{—}HC(OH)\text{—}H_2C(OH)} \rightarrow \underset{\text{glyceraldehyde}}{H_2C(OH)\text{—}HC(OH)\text{—}CHO} + 2H^+ + 2e^- \tag{1}$$

$$\underset{\text{glycerol}}{H_2C(OH)\text{—}HC(OH)\text{—}H_2C(OH)} \rightarrow \underset{\text{dihydroxyacetone}}{H_2C(OH)\text{—}CO\text{—}H_2C(OH)} + 2H^+ + 2e^- \tag{1'}$$

$$\underset{\text{glyceraldehyde}}{H_2C(OH)\text{—}HC(OH)\text{—}CHO} \xrightarrow{H_2O} \underset{\text{carboxylic acids}}{\text{R-COOH}} \tag{2}$$

$$\underset{\text{dihydroxyacetone}}{H_2C(OH)\text{—}CO\text{—}H_2C(OH)} \xrightarrow{H_2O} \underset{\text{carboxylic acids}}{\text{R}'\text{-COOH}} \tag{2'}$$

$$\underset{\text{carboxylic acids}}{\text{R-COOH}} \rightarrow \underset{\text{carbon dioxide}}{CO_2} \tag{3}$$

where R represents 0, 1 and 2 carbon atoms chains and R′ represents 2 carbon atoms chains.

Here, the adsorbed intermediates of electro-oxidation of glycerol on Pt are not represented. Steps (1) and (1′) correspond to the formation of glyceraldehyde and dihydroxyacetone, respectively. Both of them involve the production of $2H^+$ and $2e^-$. Glyceraldehyde and dihydroxyacetone can diffuse to the bulk of the solution or, alternatively, be further oxidized. The oxidation of glyceraldehyde and dihydroxyacetone to carboxylic acids [Steps (2) and (2′)] or CO_2 [Step (3)] requires the presence of oxygenated species from water splitting.

In the present work, we will generally refer to carboxylic acids, glyceraldehyde and dihydroxyacetone as carbonyl containing compounds, since we are not able to distinguish them based on our FTIR results, presented in Section 3.3.